Journal of Alloys and Compounds 480 (2009) 120–122

Contents lists available at ScienceDirect

Journal of Alloys and Compounds

journal homepage: www.elsevier.com/locate/jallcom

X-ray absorption spectroscopic analysis of $CuIr_2S_4$

N. Kijima[a,*], H. Yashiro[b], J. Awaka[a], J. Akimoto[a], S. Nagata[c]

[a] National Institute of Advanced Industrial Science and Technology (AIST), Tsukuba Central 5, 1-1-1 Higashi, Tsukuba, Ibaraki 305-8565, Japan
[b] Rigaku Corporation, 3-9-12 Matsubara-cho, Akishima, Tokyo 196-8666, Japan
[c] Department of Materials Science and Engineering, Muroran Institute of Technology, 27-1 Mizumoto-cho, Muroran, Hokkaido 050-8585, Japan

ARTICLE INFO

Article history:
Received 30 June 2008
Received in revised form
20 September 2008
Accepted 22 September 2008
Available online 22 November 2008

Keywords:
Transition metal alloys and compounds
Solid state reactions
Electronic properties
X-ray absorption fine structure

ABSTRACT

The thiospinel $CuIr_2S_4$ undergoes a temperature-induced metal–insulator transition around 230 K with structure transformation. We report on the results of X-ray absorption fine structure (XAFS) studies at the Cu K-edge and Ir L_{III}-edge of $CuIr_2S_4$. X-ray absorption spectra were measured by a laboratory XAFS apparatus over the temperature range from 50 to 300 K. The Cu K-edge X-ray absorption near edge structure (XANES) spectra verified that Cu in $CuIr_2S_4$ is monovalent, whereas Cu in spinel-type oxide $CuRh_2O_4$ is divalent. Chemical shift of Ir L_{III}-edge XANES spectrum of $CuIr_2S_4$ was larger than $IrCl_3$, and smaller than IrO_2. This finding supports the presence of both Ir^{3+} and Ir^{4+} in $CuIr_2S_4$.

1. Introduction

The spinel compounds, CuM_2X_4 (M = Rh, Ir; X = O, S, Se), have a large variety of physical properties. In particular, the thiospinel $CuIr_2S_4$ exhibits a phase transition from a paramagnetic metal to a diamagnetic insulator at around 230 K with structural transformation, showing hysteresis on heating and cooling [1]. This metal–insulator transition (MIT) has attracted much interest because of a rare example of an orbital-induced Peierls transition in a three-dimensional structure. On the other hand, $CuIr_2Se_4$ shows a metallic conductivity down to 0.5 K [1], and $CuIr_2O_4$ has not been reported as far as we know. Rh-based spinel compounds, $CuRh_2O_4$ exhibits an antiferromagnetic transition at the Néel temperature of 21.9 K [2], and both $CuRh_2S_4$ and $CuRh_2Se_4$ become superconducting below transition temperatures of 4.70 K and 3.48 K, respectively [3,4].

Among these spinel compounds, $CuIr_2S_4$ and $CuRh_2O_4$ undergo structure transformations. Our X-ray diffraction study verified that $CuRh_2O_4$ shows a first-order phase transition from a tetragonal to a cubic structure at around 850 K. This phase transition is because of the Jahn–Teller effect for Cu^{2+} ($3d^9$) ions. On the other hand, the crystal structure of low temperature phase of $CuIr_2S_4$ was subject of controversy, whereas the high temperature phase has a normal spinel structure with cubic symmetry. Later structural analysis of the low temperature phase concludes that the crystal symmetry is triclinic [5], as Fig. 1 depicts.

Several experimental techniques, e.g., electrical conductivity, magnetic susceptibility, Mössbauer spectroscopy, nuclear magnetic resonance (NMR), X-ray photoemission spectroscopy (XPS), have been applied to investigate the MIT of $CuIr_2S_4$ [1]. We report here the X-ray absorption fine structure (XAFS) studies at Cu K-edge and Ir L_{III}-edge of $CuIr_2S_4$.

2. Experimental

Reagent-grade Cu_2O (99.9%), CuO (99.9%), Rh_2O_3 (99.9%), IrO_2 (99.9%), $IrCl_3$ (99.9%), Cu (99.99%), Ir (99.99%), and S (99.9999%) were purchased from Furuuchi Chemical Corporation, which were used as starting materials for sample preparations and reference materials for XAFS measurements without further purifications. $CuIr_2S_4$ was obtained from the powdered elements of Cu, Ir, and S. These elements were mixed with nominal stoichiometry, where 0.1 mass % excess S was added. This mixture was heated in sealed quartz tubes ($\approx 10^{-5}$ Pa) to 1123 K with heating rate of 100 K/h and then kept at this temperature for 240 h. After furnace cooling, the product was reground, heated again to 1123 K, and kept for 240 h. $CuRh_2O_4$ was prepared by a solid state reaction. The starting materials, CuO and Rh_2O_3, were mixed in a stoichiometric ratio. This mixture was heated to 1173 K for 24 h in a quartz boat under air. After crushing the product, this heating was usually repeated once.

The identification of the crystal structure and the determination of the lattice constant were carried out by the powder X-ray diffraction (XRD) method. XRD data were taken with Cu Kα radiation on a Bragg–Brentano-type powder diffractometer (Rigaku RINT-2550VHF) at room temperature. The X-ray absorption spectra were measured with a laboratory XAFS apparatus (Rigaku R-EXXAFS Super) over the temperature range from 50 to 300 K. All the samples were ground to fine powders, and then covered uniformly on an adhesive tape, which was folded into some layers to obtain an optimum absorption jump. All the data were recorded with a spacing of

---

* Corresponding author.
E-mail address: n-kijima@aist.go.jp (N. Kijima).

0925-8388/$ – see front matter © 2008 Elsevier B.V. All rights reserved.
doi:10.1016/j.jallcom.2008.09.199

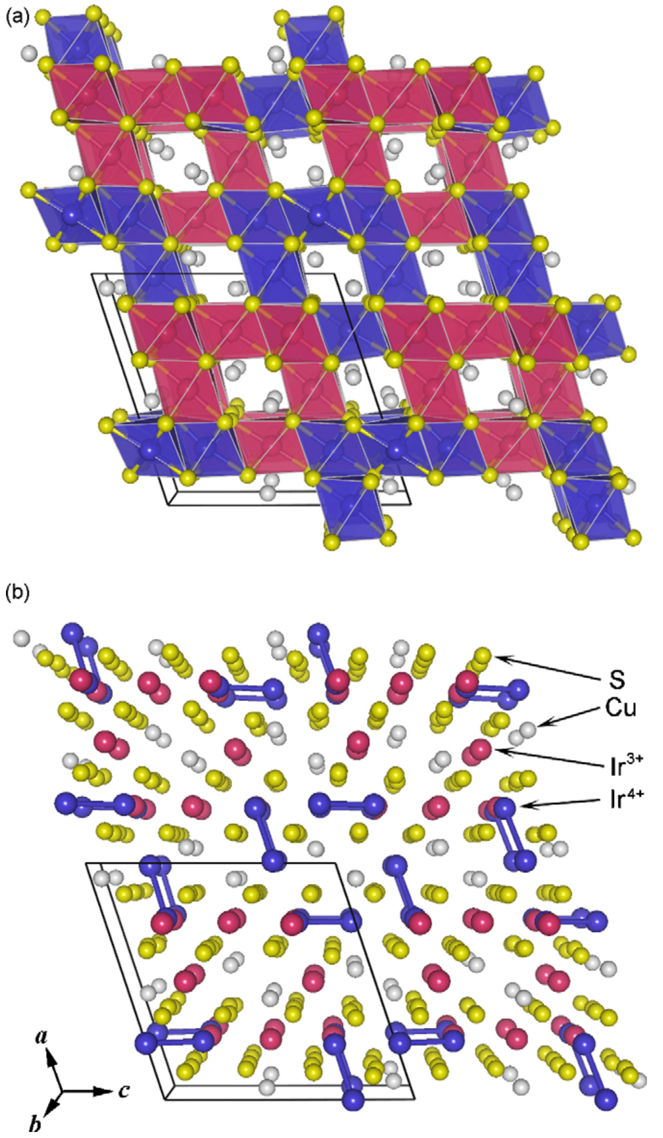

Fig. 1. Crystal structure of low temperature phase of $CuIr_2S_4$. (a) Red and blue IrS_6 octahedra have Ir^{3+} and Ir^{4+}, respectively. (b) The dimerized Ir^{4+}–Ir^{4+} bonds are indicated with blue cylinders. The crystal structure data were taken from supplementary information in Ref. [5]. (For interpretation of the references to color in this figure legend, the reader is referred to the web version of the article.)

1.0 eV in a transmission mode. The REX2000 [6] computer program was used for the analysis of the XAFS data.

3. Results and discussion

Both $CuIr_2S_4$ and $CuRh_2O_4$ samples prepared were confirmed to be single-phases by XRD. The $CuIr_2S_4$ sample obtained was of cubic symmetry ($Fd\text{-}3m$, no.227) with lattice constant of $a = 9.8509(12)$ Å at room temperature. The $CuRh_2O_4$ sample had tetragonal symmetry ($I4_1/amd$, no.141) with lattice constant of $a = 6.174(3)$ Å and $c = 7.911(5)$ Å at room temperature. In addition, reference materials for XAFS measurements, Cu_2O, CuO, IrO_2, $IrCl_3$, were also single-phases.

Fig. 2 shows Cu K-edge and Ir L_{III}-edge X-ray absorption near-edge structure (XANES) spectra of $CuIr_2S_4$ and reference materials at 300 K. The chemical shifts for the specimens were estimated by the procedure as a zero intercept in a plot of absorption versus energy. As Fig. 2(a) demonstrates, Cu K-edge XANES spectra verified that Cu in $CuIr_2S_4$ is monovalent because chemical shift of $CuIr_2S_4$ agrees with that of Cu_2O. This finding is consistent with result of previous NMR [7], XPS [8], and band-structure calculations [9]. In contrast, Cu in $CuRh_2O_4$ is divalent, which is also consistent with the antiferromagnetic behavior due to Cu^{2+} ($3d^9$, $S = 1/2$) ions [2]. The valence state of Cu in the spinel compounds distinctly differs between the oxide and the sulfide. On the other hand, chemical shift of Ir L_{III}-edge XANES spectrum of $CuIr_2S_4$ was larger than $IrCl_3$, and smaller than IrO_2, as Fig. 2(b) shows. This finding supports that Ir forms a mixed valence state of Ir^{3+} and Ir^{4+} which is responsible for metallic conduction in the cubic phase of $CuIr_2S_4$. Croft et al. also measured the L_{III}-edge XANES spectra of Ir, IrO_2, and $CuIr_2S_4$ at room temperature [10]. Their spectra are consistent with our spectra.

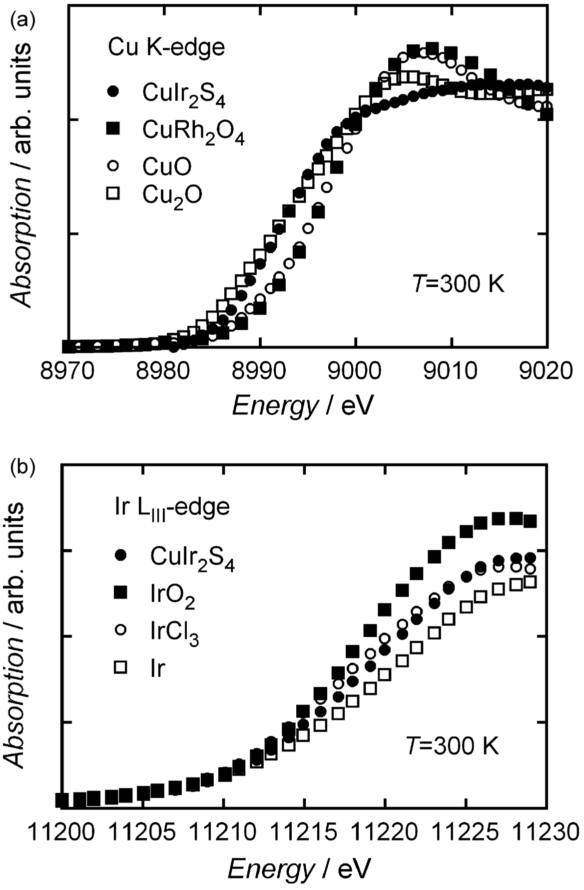

Fig. 2. (a) Cu K-edge XANES spectra of $CuIr_2S_4$, $CuRh_2O_4$, CuO, and Cu_2O; (b) Ir L_{III}-edge XANES spectra of $CuIr_2S_4$, IrO_2, $IrCl_3$, and Ir at 300 K.

Fig. 3 shows Cu K-edge and Ir L_{III}-edge XANES spectra of $CuIr_2S_4$ at 50 K, 100 K, 200 K, and 300 K. Cu K-edge XANES spectra were almost independent on the temperatures across the MIT. On the other hand, Ir L_{III}-edge XANES spectra is slightly shifted to the higher energy side below the MIT temperature. This observation would be reflected to the Ir electronic state redistribution across the MIT. In prior work [10], Croft et al. reported the significant changes of *S* K-edge XANES spectra of $CuIr_2S_4$ across the MIT. They propose that the dimerization due to charge and orbital ordering is responsible for the electronic structural change [10].

$CuIr_2S_4$ is a diamagnetic insulator below the MIT temperature, where Cu ion is Cu^{1+} and Ir has mixed valence state of Ir^{3+} and Ir^{4+}. In the diamagnetic insulator phase, the dimerization of Ir^{4+}–Ir^{4+} having $S = 0$ is formed [1,5,10], and Ir^{3+} is non-magnetic state with t_{2g}^6 occupation. The dimerized Ir^{4+}–Ir^{4+} bonds are highlighted in Fig. 1. To make clear interatomic distance in $CuIr_2S_4$ across the MIT, we performed extended X-ray absorption fine structure (EXAFS)

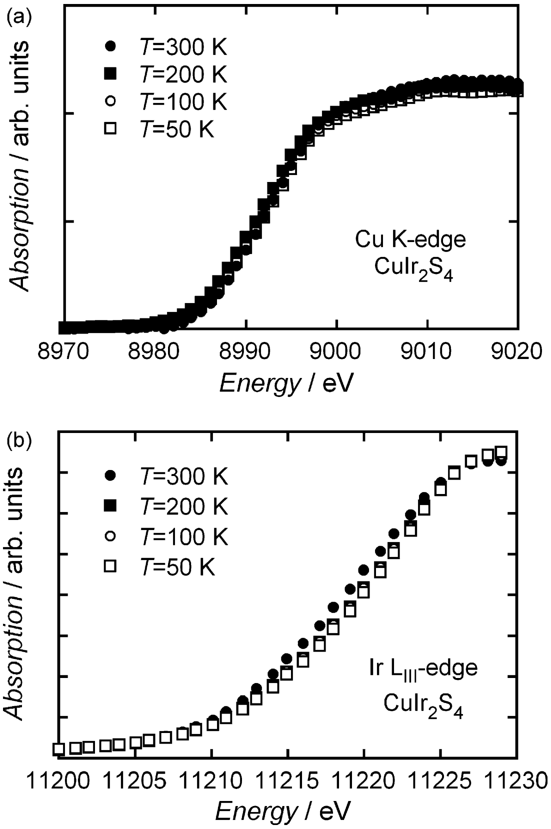

Fig. 3. (a) Cu K-edge and (b) Ir L_{III}-edge XANES spectra of $CuIr_2S_4$ at 50 K, 100 K, 200 K, and 300 K.

measurement. The Fourier transformation of Ir L_{III}-edge EXAFS oscillation functions were carried out, which is not given as the figure in this report. The peak around 2 Å corresponding to Ir–S distance was obtained clearly. The Ir–S distance was almost independent on the temperatures across the MIT. On the other hand, a peak corresponding to Ir–Ir distance could not be detected obviously within our resolution. The observation of Ir^{4+}–Ir^{4+}dimer by EXAFS experiments would be difficult.

In summary, our XAFS studies verified that Cu is monovalent and Ir forms a mixed valence state of Ir^{3+} and Ir^{4+} in $CuIr_2S_4$. The Ir L_{III}-edge XANES spectra is slightly shifted across the MIT, although Cu K-edge XANES spectra were almost independent on the temperature.

Acknowledgement

We thank Dr. Mastumoto (AIST) and Dr. Endoh (Toray Research Center, Inc.) for their valuable discussion.

References

[1] S. Nagata, Chin. J. Phys. 43 (2005) No. 3-II, 722 and references therein.
[2] R. Endoh, O. Fujishima, T. Atake, N. Matsumoto, M. Hayashi, S. Nagata, J. Phys. Chem. Solids 60 (1999) 457.
[3] T. Hagino, Y. Seki, N. Wada, S. Tsuji, T. Shirane, K. Kumagai, S. Nagata, Phys. Rev. B 51 (1995) 12673.
[4] N. Kijima, H. Yashiro, S. Nagata, J. Phys. Chem. Solids 57 (1996) 1635.
[5] P.G. Radaelli, Y. Horibe, M.J. Gutmann, H. Ishibashi, C.H. Chen, R.M. Ibberson, Y. Koyama, Y.-S. Hor, V. Kiryukhin, S.-W. Cheong, Nature (London) 416 (2002) 155.
[6] Rigaku, EXAFS analysis software, REX2000, Cat. no. 2612S311/S312/S313/S321/S321/S322/S323, Rigaku, Co., 2003.
[7] S. Tsuji, K. Kumagai, N. Matsumoto, S. Nagata, Physica C 282-287 (1997) 1107.
[8] J. Matsuno, T. Mizokawa, A. Fujimori, D.A. Zatsepin, V.R. Galakhov, E.Z. Kurmaev, Y. Kato, S. Nagata, Phys. Rev. B 55 (1997) R15979.
[9] T. Oda, M. Shirai, N. Suzuki, K. Motizuki, J. Phys. Condens. Mater. (1995) 4433.
[10] M. Croft, W. Caliebe, H. Woo, T.A. Tyson, D. Sills, Y.S. Hor, S.-W. Cheong, V. Kiryukhin, S.-J. Oh, Phys. Rev. B 67 (2003) 201102.